# Quantum Corrections in Nanoplasmonics: Shape, Scale, and Material

Thomas Christensen,[1,*] Wei Yan,[2,†] Antti-Pekka Jauho,[3,4] Marin Soljačić,[1] and N. Asger Mortensen[3,5]

[1]*Department of Physics, Massachusetts Institute of Technology, Cambridge, Massachusetts 02139, USA*
[2]*Institut d'Optique d'Aquitaine, Université Bordeaux, CNRS, 33405 Talence, France*
[3]*Center for Nanostructured Graphene, Technical University of Denmark, DK-2800 Kongens Lyngby, Denmark*
[4]*Department of Micro- and Nanotechnology, Technical University of Denmark, DK-2800 Kongens Lyngby, Denmark*
[5]*Department of Photonics Engineering, Technical University of Denmark, DK-2800 Kongens Lyngby, Denmark*

The classical treatment of plasmonics is insufficient at the nanometer-scale due to quantum mechanical surface phenomena. Here, an extension of the classical paradigm is reported which rigorously remedies this deficiency through the incorporation of first-principles surface response functions—the Feibelman $d$ parameters—in general geometries. Several analytical results for the leading-order plasmonic quantum corrections are obtained in a first-principles setting; particularly, a clear separation of the roles of shape, scale, and material is established. The utility of the formalism is illustrated by the derivation of a modified sum rule for complementary structures, a rigorous reformulation of Kreibig's phenomenological damping prescription, and an account of the small-scale resonance shifting of simple and noble metal nanostructures.

Classical treatments of plasmonics require specification of just two elements: geometry, involving shape and scale, and dielectric environment, supplied through local bulk dielectric functions. In the deep subwavelength regime, i.e., in the nonretarded limit, even the element of scale is rendered superfluous by scale-invariant governing equations. As the geometric scale is reduced further, below 10–20 nm in metals, toward the intrinsic quantum mechanical length scales of the plasmon-supporting electron gas, the classical approach inevitably deteriorates, as established by numerous experiments [1–10]. The main shortcomings of the classical approach can be divided into three categories [11], resulting from the neglect of (i) spill-out of the conduction electron's wave function beyond the material boundaries [12], (ii) nonlocality, i.e., the momentum dependence of the bulk response functions [13], and (iii) incomplete accounting of internal electron dynamics, especially surface-enabled plasmon damping by electron-hole pair creation [10,14]. In the subnanometer domain, additional shortcomings are expected to materialize, e.g., due to size quantization [15,16] and the breakdown of jellium treatments [17,18]. Jointly, these shortcomings and their impact on plasmonic observables (modal spectrum, field enhancements, local density of states, etc.) motivate and define the field of quantum nanoplasmonics [12,13,17].

While time-dependent density-functional theory (TDDFT) [19], in principle, can bridge the gap between classical and quantum nanoplasmonics, its explicit application is, in practice, limited to few-atom clusters and systems of high spatial symmetry due to computational constraints. A sizable fraction of nanoplasmonic structures of interest [20–22], thus, fall in a region which is simultaneously inaccessible to conventional, explicit TDDFT and beyond the validity of

classical plasmonics, roughly spanning characteristic geometric scales $L \sim 2$–20 nm. In this Letter, we provide a simple and general answer to the central question raised by this dichotomy: namely, what are the leading-order nonclassical corrections to classical plasmonics at small $L$? We find that the three main shortcomings—spill-out, nonlocality, and incompleteness—can be simultaneously overcome by extending the applicability of Feibelman's $d$ parameters [11] to general geometries; an approach which is partly inspired by a recent computational development [23]. Our simultaneous account of all three shortcomings is crucial; previous efforts to alleviate a solitary deficiency, e.g., nonlocality within the hydrodynamic model (HDM) [24–27], are limited in scope and accuracy due to an arbitrary allocation of focus among nonclassical mechanisms of comparable magnitude.

The results presented here demonstrate that the leading-order spectral corrections to classical plasmonics appear as products of material-dependent surface response functions—the Feibelman parameters $d_\perp$ and $d_\parallel$ (see Fig. 1)—and a novel set of geometry-dependent perturbation factors, $\Lambda_\perp^{(1)}$ and $\Lambda_\parallel^{(1)}$, which exhibit a $1/L$ scale dependency. The resulting formalism, which amounts to a perturbation expansion of a generalized nonretarded boundary integral equation (NBIE), is simple and amenable to analytical treatments, yet rigorous and model independent. The approach instates a natural partitioning of optical and electronic aspects, thereby indicating an advantageous division of labor in quantum nanoplasmonics between the condensed matter and optics communities.

*Feibelman d parameters.*—The classical local response (LR) description of light scattering at an interface, say, a planar interface at $x = 0$ separating metallic ($x < 0$) and dielectric ($x > 0$) regions with LR bulk dielectric functions
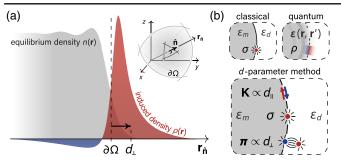
FIG. 1.    Surface features in quantum plasmonics. (a) Schematic of equilibrium and induced densities, $n(\mathbf{r})$ and $\rho(\mathbf{r})$, (distinct scales) plotted along a coordinate line, $\mathbf{r}_{\hat{\mathbf{n}}}$, normal to an $\hat{\mathbf{n}}$-oriented surface $\partial\Omega$ which delimits the ionic boundary of a metallic domain $\Omega$, see inset. Both $n(\mathbf{r})$ and $\rho(\mathbf{r})$ may extend beyond $\partial\Omega$; $d_\perp$ is the centroid of $\rho(\mathbf{r})$. (b) The leading-order differences between classical [local response, $\varepsilon_{m,d}$; induced surface density $\sigma(\partial\Omega)$] and quantum accounts [nonlocal response, $\boldsymbol{\varepsilon}(\mathbf{r},\mathbf{r}')$; induced density $\rho(\mathbb{R}^3)$] of the plasmonic response of a surface may be bridged by introducing nonclassical contributions due to surface dipole and current densities, $\boldsymbol{\pi}(\mathbf{r})$ and $\mathbf{K}(\mathbf{r})$, proportional to the Feibelman parameters $d_\perp$ and $d_\parallel$, respectively, which originate from a dipole expansion of $\rho(\mathbf{r})$.

$\varepsilon_m(\omega)$ and $\varepsilon_d(\omega)$, respectively, implies that the induced charge density, $\rho(\mathbf{r})$, is confined strictly to the interface such that $\rho(\mathbf{r}) = \delta(x)\sigma(y,z)$. The classical treatment consequently amounts to a monopole approximation of the nonsingular quantum mechanical $\rho(\mathbf{r})$, see Fig. 1. As demonstrated in Feibelman's seminal work on planar semi-infinite systems [11], the first-order extension of this zeroth-order multipole expansion naturally introduces two auxiliary quantities, $d_\perp$ and $d_\parallel$, which parametrize the first moments of the induced charge and current density, $\mathbf{J}(\mathbf{r})$. A self-contained introduction to their properties is provided in the Supplemental Material (SM) [28]. In brief, they represent model-dependent (e.g., TDDFT or HDM) surface-response functions, and provide the leading-order corrections to classicality. Formally, for an external exciting potential $\phi^{\text{ext}}(\mathbf{r}) = e^{iky+kx}$ oscillating at frequency $\omega$, they follow directly from the induced dynamic quantities $\rho(\mathbf{r}) = \rho(x)e^{iky}$ and $\mathbf{J}(\mathbf{r}) = \mathbf{J}(x)e^{iky}$ [44]:

$$d_\perp = \frac{\int_{-\infty}^{\infty} x\rho(x)\,dx}{\int_{-\infty}^{\infty} \rho(x)\,dx}, \qquad d_\parallel = \frac{\int_{-\infty}^{\infty} x\frac{\partial}{\partial x}\mathbf{J}_y(x)\,dx}{\int_{-\infty}^{\infty} \frac{\partial}{\partial x}\mathbf{J}_y(x)\,dx}. \qquad (1)$$

Both quantities define a characteristic length scale of the dynamic problem: the centroid of induced charge ($d_\perp$) and of the normal derivative of tangential current ($d_\parallel$) [45]. Equivalently, they can be cast as derivatives of moments of the nonlocal dielectric tensor $\boldsymbol{\varepsilon}(\mathbf{r},\mathbf{r}')$ of the semi-infinite planar system, see SM [28]. Notably, $d_\parallel$ vanishes for neutral strictly planar interfaces [44,46], leaving $d_\perp$ as the main quantity of interest for intrinsic quantum mechanical corrections; nevertheless, $d_\parallel$ is retained since it facilitates

treatment of surface roughness [47], excess surface charge, e.g., due to adsorption, and semiclassical accounts of bound screening [48]. Lastly, the $d$ parameters are implicit functions of both $k$ and $\omega$; the $k$ dependence, however, is weak [23] and, furthermore, contributes only at second order in deviations from classicality, as observed first by Apell and Ljungbert [49,50]. Crucially, this facilitates a mapping of local ($k \to 0$) $d$ parameters of planar interfaces to general, curved geometries. This freedom of mapping is the central notion which allows the ensuing considerations [51].

*Governing equations.*—The classical NBIE [52–54] amounts to the solution of a scalar integral equation in an unknown surface charge density $\sigma(\mathbf{r},\omega)$ over a (possibly disconnected) surface domain $\mathbf{r} \in \partial\Omega$, separating an interior metallic domain $\Omega$, with outward normal $\hat{\mathbf{n}}$, from an exterior dielectric domain. It constitutes a natural point of departure because it explicates the distinct and decoupled roles of material and shape as well as the scale-invariance of classical nonretarded treatments. The extension to account for surface contributions due to $d_\perp$ and $d_\parallel$ follows by including two distinct polarizable boundary layers, see SM [28], one carrying a dipole density $\boldsymbol{\pi}(\mathbf{r},\omega) \equiv d_\perp(\omega)\sigma(\mathbf{r},\omega)\hat{\mathbf{n}}$ and one carrying a surface current $\mathbf{K}(\mathbf{r},\omega) \equiv s(\omega)\mathbf{E}_\parallel(\mathbf{r},\omega)$ proportional to the tangential electric field $\mathbf{E}_\parallel \equiv (\mathbf{I} - \hat{\mathbf{n}}\,\hat{\mathbf{n}})\mathbf{E}$ and a surface conductivity $s(\omega) \equiv i\varepsilon_0(\varepsilon_d - \varepsilon_m)\omega d_\parallel(\omega)$. The integral equation consistent with these additional terms is derived in the SM [28], and yields a generalized NBIE ($\omega$ dependence implicit)

$$\Lambda\sigma(\mathbf{r}) = \mathrm{P}\int_{\partial\Omega} [\hat{\mathbf{n}} \cdot \boldsymbol{\nabla}g(\mathbf{r},\mathbf{r}')]\sigma(\mathbf{r}')\,d^2\mathbf{r}'$$
$$+ d_\perp \lim_{\delta\to 0^+} \int_{\partial\Omega} [\hat{\mathbf{n}} \cdot \boldsymbol{\nabla}\boldsymbol{\nabla}'g(\mathbf{r}+\delta\hat{\mathbf{n}},\mathbf{r}') \cdot \hat{\mathbf{n}}']\sigma(\mathbf{r}')\,d^2\mathbf{r}'$$
$$- d_\parallel \int_{\partial\Omega} \nabla_\parallel^2 g(\mathbf{r},\mathbf{r}')\sigma(\mathbf{r}')\,d^2\mathbf{r}', \qquad (2)$$

with scalar Coulomb interaction $g(\mathbf{r},\mathbf{r}') \equiv 1/2\pi|\mathbf{r}-\mathbf{r}'|$, Cauchy principal value P, surface Laplacian $\nabla_\parallel^2$, and dimensionless eigenvalue $\Lambda \equiv (\varepsilon_d + \varepsilon_m)/(\varepsilon_d - \varepsilon_m)$ parametrized by the frequency-dependent LR bulk dielectric functions of the constituent materials. Equation (2) may equivalently be written in operator form as $\Lambda|\sigma\rangle = (\mathsf{K} + d_\alpha\mathsf{V}_\alpha)|\sigma\rangle$, with operators $\mathsf{K}$ and $d_\alpha\mathsf{V}_\alpha$ (implicitly summed over $\alpha = \{\perp,\parallel\}$) acting on ket states $\langle\mathbf{r}|\sigma\rangle \equiv \sigma(\mathbf{r})$. The classical operator $\mathsf{K}$ is scale invariant, cf. its nondimensionalized form. Accordingly, the classical eigenproblem $\Lambda^{(0)}|\sigma^{(0)}\rangle = \mathsf{K}|\sigma^{(0)}\rangle$ is solely shape dependent, and its dimensionless eigenvalues $\Lambda^{(0)}$ constitute plasmonic shape factors. Conversely, the nonclassical operators $\mathsf{V}_\alpha$ exhibit an inverse scale dependency $\propto 1/L$, thereby, introducing scale-invariance breaking of magnitude $d_\alpha/L$. Even so, for small but non-negligible breaking, the spectral properties remain expressible in terms of shape factors, as we demonstrate in the following.

*Nonclassical geometry-dependent corrections.*—The eigensolutions $\{\Lambda_n^{(0)}, |\sigma_n^{(1)}\rangle\}$ of $\mathsf{K}$, and their associated surface potentials $|\phi_n^{(0)}\rangle \equiv (2\varepsilon_0)^{-1}\mathsf{g}|\sigma_n^{(0)}\rangle$ [with $\langle\mathbf{r}|\mathsf{g}|\mathbf{r}'\rangle \equiv g(\mathbf{r},\mathbf{r}')$] form a biorthogonal basis over $\partial\Omega$ such that $\langle\phi_n^{(0)}|\sigma_{n'}^{(0)}\rangle \propto \delta_{nn'}$ [53]. In seeking the leading order corrections to $\Lambda^{(0)}$ due to $d_\alpha V_\alpha$, we may consequently apply perturbation theory around these classical eigensolutions. Specifically, writing the perturbed eigenvalue $\Lambda$ as (eigenindex $n$ implicit)

$$\Lambda = \Lambda^{(0)} + \Lambda_\alpha^{(1)}d_\alpha + O(d_\alpha^2), \tag{3a}$$

introduces geometry-dependent perturbation factors $\Lambda_\alpha^{(1)} \equiv \langle\phi^{(0)}|V_\alpha|\sigma^{(0)}\rangle/\langle\phi^{(0)}|\sigma^{(0)}\rangle$ which simplify to (see SM [28])

$$\Lambda_\perp^{(1)} = \frac{(\Lambda^{(0)})^2 - 1}{2\varepsilon_0}\frac{\langle\sigma^{(0)}|\sigma^{(0)}\rangle}{\langle\phi^{(0)}|\sigma^{(0)}\rangle}, \tag{3b}$$

$$\Lambda_\parallel^{(1)} = 2\varepsilon_0\frac{\langle\boldsymbol{\nabla}_\parallel\phi^{(0)}|\boldsymbol{\nabla}_\parallel\phi^{(0)}\rangle}{\langle\phi^{(0)}|\sigma^{(0)}\rangle}. \tag{3c}$$

We note the following features of $\Lambda_{\perp,\parallel}^{(1)}$: (i) their unit is inverse length, i.e., they represent effective wave numbers analogous to $k$ in the planar semi-infinite system; (ii) non-dimensionalization reveals a factorizable form $\Lambda_\alpha^{(1)} = \tilde{\Lambda}_\alpha^{(1)}/L$ in terms of a dimensionless shape factor $\tilde{\Lambda}_\alpha^{(1)}$ and a characteristic scale $1/L$; and (iii) $\Lambda_\perp^{(1)} < 0$ and $\Lambda_\parallel^{(1)} > 0$, see SM [28].

The perturbation result for $\Lambda$, Eqs. (3), allows a concomitant spectral statement. Specifically, for a classical eigenfrequency $\omega^{(0)} \equiv \omega(\Lambda^{(0)})$, the first-order spectral correction $\omega \equiv \omega^{(0)} + \omega^{(1)} + O((\omega - \omega^{(0)})^2)$ follows by expanding Eq. (3a) around $\omega^{(0)}$

$$\omega^{(1)} = \frac{\Lambda_\alpha^{(1)}d_\alpha^{(0)}}{\frac{\partial}{\partial\omega}(\Lambda - \Lambda_\alpha^{(1)}d_\alpha)^{(0)}} \simeq \frac{\Lambda_\alpha^{(1)}d_\alpha^{(0)}}{(\frac{\partial}{\partial\omega}\Lambda)^{(0)}}, \tag{4}$$

here, the second approximate equality neglects the dispersion of $d_\alpha(\omega)$, i.e. a pole approximation, and the superscript (0) indicates evaluation at the classical frequency $\omega^{(0)}$, such that, e.g., $d_\alpha^{(0)} \equiv d_\alpha(\omega^{(0)})$. The result is particularly elucidating for the lossless homogeneous electron gas (HEG) in vacuum [$\varepsilon_d = 1$, $\varepsilon_m(\omega) = 1 - \omega_p^2/\omega^2$, and $\omega^{(0)} = \omega_p\sqrt{(1 + \Lambda^{(0)})/2}$], reducing there to $\omega^{(1)} = \frac{1}{4}\Lambda_\alpha^{(1)}d_\alpha^{(0)}\omega_p^2/\omega^{(0)}$. Since $\Lambda_\perp^{(1)} < 0$ resonances consequently redshift (blueshift) if $d_\perp^{(0)} > 0$ ($< 0$), paralleling the results of the planar interface. Conversely, the sign of $d_\parallel^{(0)}$ indicates shifting in the opposite direction since $\Lambda_\parallel^{(1)} > 0$.

In systems of sufficiently high symmetry, the perturbative results, i.e., Eqs. (3), coincide with exact solutions of Eq. (2) since first- and higher-order corrections to $|\sigma\rangle = |\sigma^{(0)}\rangle + |\sigma^{(1)}\rangle + \cdots$ vanish by symmetry constraints. Table I lists exact analytical results for a number of such sufficiently symmetric systems, derived using suitable modal expansions of the Coulomb interaction, see SM [28]. The results for the half-space and sphere reproduce the special cases previously obtained by Feibelman [11] and Apell and Ljungbert [49,50], respectively. The generality of the present approach additionally allows the derivation of new analytical results, here exemplified for the cylinder, slab, and gap geometries. The utility and universality of the present approach is further illustrated by the fact that Eqs. (3) and (4), and Table I, in particular, readily reproduce all known first-order HDM results [55,56] when the HDM approximation of the $d$ parameters is employed [57], i.e., when $d_\parallel^{\text{HDM}} = 0$ and $d_\perp^{\text{HDM}}(\omega) = -\beta/(\omega_p^2 - \omega^2)^{1/2}$ with $\beta^2 \equiv \frac{3}{5}v_F^2$ [11].

In less symmetric geometries, analytical solutions cannot generally be obtained. Regardless, the classical NBIE operator $\mathsf{K}$ can be discretized by the boundary element method [54] allowing the numerical calculation of the nonclassical shape factors $\tilde{\Lambda}_\alpha^{(1)} = \Lambda_\alpha^{(1)}L$ via Eqs. (3). Figure 2 presents the results of such a calculation, here, for the dipolar modes of experimentally relevant geometries over a range of aspect ratios $a/b$, specifically for cubes, pills, spheroids, and triangles. The former three reduce to spheres at aspect ratios $a/b = 2$, 1, and 1, respectively. Interestingly, though the $a/b$ dependence of the classical dipole eigenvalue $\Lambda^{(0)}$ is qualitatively similar across the

TABLE I. Analytical eigenvalues $\Lambda \equiv \Lambda^{(0)} + d_\perp\Lambda_\perp + d_\parallel\Lambda_\parallel$ of Eq. (2) valid to all orders in $d_\alpha$. The metallic geometries (and associated geometric length scales) are indicated schematically in gray; the relevant eigenindices are, from top to bottom, wave number $k$, symmetric (upper sign) and antisymmetric (lower sign) charge density parity, polar angular momentum $l$, azimuthal angular momentum $m$, and dimensionless axial wave number $\tilde{k} \equiv kR$. $K_m$ and $I_m$ denote modified Bessel functions.

| Geometry | $\Lambda^{(0)}$ | $\Lambda_\perp$ | $\Lambda_\parallel$ |
|---|---|---|---|
| half-space | $0$ | $-k$ | $k$ |
| slab | $\mp e^{-kt}$ | $-(1\mp e^{-kt})k$ | $(1\pm e^{-kt})k$ |
| gap | $\pm e^{-kt}$ | $-(1\mp e^{-kt})k$ | $(1\pm e^{-kt})k$ |
| sphere | $-\dfrac{1}{2l+1}$ | $-\dfrac{2l(l+1)}{(2l+1)R}$ | $\dfrac{2l(l+1)}{(2l+1)R}$ |
| cylinder | $\tilde{k}[K_m(\tilde{k})I_m(\tilde{k})]'$ | $\dfrac{(\Lambda^{(0)})^2-1}{2K_m(\tilde{k})I_m(\tilde{k})R}$ | $2K_m(\tilde{k})I_m(\tilde{k})\dfrac{m^2+\tilde{k}^2}{R}$ |

considered shapes, e.g., monotonically decreasing with $a/b$, the corresponding dependence of $\Lambda_\alpha^{(1)}$ is markedly dissimilar for distinct shapes. In this sense, nonclassicality constitutes a stronger probe of local geometric features than its underlying classical correspondent.

*Breaking of classical complementarity.*—The classical NBIE naturally leads to a nonretarded spectral sum rule for the resonances of complementary geometries (i.e., of interchanged material regions) [59]. Concretely, the equimodal (i.e., of identical modal pattern) eigenvalues of a region $\Omega$ and its complement $\Omega^{\complement} \equiv \mathbb{R}^3 \backslash \Omega$, denoted $\Lambda^{(0)}$ and $\Lambda^{(0),\complement}$, respectively, are interrelated by $\Lambda^{(0)} = -\Lambda^{(0),\complement}$, since $\Omega$ and $\Omega^{\complement}$ are distinguished in the NBIE only by the sign of the surface normal $\hat{\mathbf{n}}$ [59]. This is the classical statement of complementarity in the small-scale limit. The present extension of the NBIE allows a refinement of this statement; specifically, it follows from the absence of an $\hat{\mathbf{n}}$ dependence in Eqs. (3) that $\Lambda_\alpha^{(1)} = \Lambda_\alpha^{(1),\complement}$ (this fact is exemplified, e.g., by the slab and gap results of Table I). Consequently, classical complementarity is broken in the sense

$$\Lambda + \Lambda^{\complement} = \Lambda_\alpha^{(1)}(d_\alpha + d_\alpha^{\complement}) + O(d_\alpha^2), \quad (5)$$

with $d_\alpha^{(\complement)}$ evaluated at $\omega^{(\complement)}$. For the HEG in vacuum, this entails a modified sum rule $\omega^2 + (\omega^{\complement})^2 \simeq \omega_p^2 [1 + \frac{1}{2}\Lambda_\alpha^{(1)}(d_\alpha + d_\alpha^{\complement})]$. This new finding establishes that classical complementarity is generically broken, even in the small-scale limit; it is attained only approximately in an intermediate domain
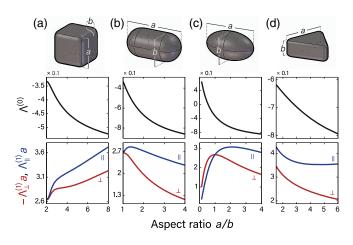


FIG. 2. Aspect ratio dependence, $a/b$, of the shape factors, $\Lambda^{(0)}$, $-\Lambda_\perp^{(1)}a$, and $\Lambda_\parallel^{(1)}a$ (the latter two normalized by the length $L = a$) for four canonical geometries: (a) cubes of side $a$ and edge- and corner-rounding $2b$, (b) cylindrical pills of length $a$, diameter $b$, and butt-rounding $b$, (c) spheroids with principal axis $a$ and $b$, and (d) equilateral triangles of height $b$, side $a$, and edge- and corner-rounding $\approx 0.165a$. A dipole mode is considered in all cases; its induced dipole is along $a$ in (a)–(c) and along the triangle altitude in (d). Rounding is intramural and of cylindrical and spherical kind with inscribed diameters equaling the specified rounding value.

bounded by large- and small-scale breakings due to retardation ($\varpropto L$) and nonclassical surface effects ($\varpropto 1/L$). A prior HDM study of the slab-gap system exemplifies a special case of this result [60].

*Surface-enhanced plasmon decay.*—Finally, we discuss the size-dependent decay of plasmons. Equation (4) directly facilitates a rigorous treatment of this aspect; in particular, splitting the imaginary part of a resonance frequency $\text{Im}\,\omega \equiv -\frac{1}{2}(\gamma^{(0)} + \gamma^{(1)})$ into a classical part $\gamma^{(0)}$ due to bulk absorption and a nonclassical part $\gamma^{(1)}$ due to surface-enabled absorption, we find (assuming $\text{Re}\,\omega \gg \gamma^{(0,1)}$)

$$\gamma^{(1)} \simeq -2\frac{\Lambda_\alpha^{(1)}\text{Im}\,d_\alpha^{(0)}}{\text{Re}\,(\frac{\partial}{\partial\omega}\Lambda)^{(0)}} \simeq -\frac{1}{2}\frac{\omega_p^2}{\text{Re}\,\omega^{(0)}}\Lambda_\alpha^{(1)}\text{Im}\,d_\alpha^{(0)}, \quad (6)$$

specializing at the last equality to the HEG in vacuum. This result generalizes the well-known phenomenological Kreibig approach often adopted in nanospheres, which takes $\gamma^{(1)} \sim v_F/R$ [61,62] extending its applicability to arbitrary geometries [63]. Similarly, it provides a first-principles alternative to the recently proposed diffusive HDM [64].

These considerations are further expounded in Fig. 3 for HEGs of Wigner-Seitz radius $r_s = 2$ and 4 (qualitatively representative of Al and Na, respectively) and Ag. Figure 3(a) depicts TDDFT calculations of $d_\perp$ (adopting a local exchange-correlation potential [66]). For Ag, the $5s$ orbitals are treated at the TDDFT level, while $d$-band screening is included via Liebsch's semiclassical screening approximation (SSA) (see SM [28]) [67], which necessitates inclusion of nonzero $d_\parallel$ values [48]; associated bulk properties are taken from measured data [68]. The spectral size dispersion of plasmons due to these $d$ parameters is explored in Figs. 3(b)–3(c) for a sphere, cube, and triangle, obtained by numerical solution of Eq. (3a) with shape factors from Table I and Fig. 2. The inverse scale proportionality $\omega^{(1)} \varpropto 1/L$ of Eq. (4) is clearly displayed for both real and imaginary parts regardless of material, being only slightly modified at the smallest considered scale due to spectral dispersion of $d_\alpha$. The $r_s = 4$ nanosphere is compared with explicit TDDFT calculations of $\text{Re}\,\omega$ by Weick *et al.* [65]; excellent agreement is observed (enduring at even smaller radii as well, see SM [28]). In the HEGs, all considered geometries incur redshifting $\text{Re}\,\omega$ since $d_\perp(\omega^{(0)}) > 0$; conversely, the interplay between $d_\perp$ and $d_\parallel$ manifests itself as a blueshift for the Ag sphere and cube. In contrast, the Ag triangle redshifts since Ag's $d$-band screening is reduced at the lower resonance frequency of the triangle, tending there to a HEG-like response in $d_\alpha$. We note that the definiteness of this last prediction hinges on the fidelity of the SSA which, despite its merits, has shortcomings (see SM [28]); this notwithstanding, it plainly illustrates that this key
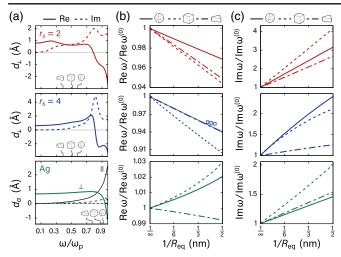
FIG. 3. The role of material, shape, and scale in the spectral properties of plasmonic nanostructures. (a) The spectral dependence of $d_\perp$ for HEGs ($r_s = 2$ and 4) and Ag ($d_\parallel$ in black). Ag is normalized by its screened plasma frequency $\hbar\omega_p = 3.81$ eV. (b)–(c) The real and imaginary part of the resonance dispersion with inverse scale, indicated by equivalent spherical radius $R_{eq} \equiv (\frac{3}{4\pi} \times \text{volume})^{1/3}$, for spheres, cubes ($a/b = 5$), and triangles ($a/b = 3$) for the materials considered in (a) with matching color code (HEGs; Drude decay $\gamma^{(0)} = \omega_p/50$). The classical resonance position $\text{Re}\,\omega^{(0)}$ of the geometries are indicated in (a) by line-connected symbols. TDDFT calculations by Weick *et al.* [65] of jellium Na nanospheres ($r_s = 3.93$) are shown in (b) by square markers.

characteristic, the nonclassical shift's sign, generally may exhibit both material and shape dependence.

*Conclusions and outlook.*—In this Letter, we have demonstrated that the rich interplay between scale, shape, and material in quantum nanoplasmonics can be understood quantitatively through just five parameters: $L$, $\tilde{\Lambda}_\alpha^{(1)}$, and $d_\alpha$. These parameters are the natural nonclassical extensions that complement the bulk dielectric functions and modal shape factor, $\varepsilon_m$, $\varepsilon_d$, and $\Lambda^{(0)}$, of classical plasmonics. They originate physically from dynamic surface dipole and current densities, $\pi(\mathbf{r})$ and $\mathbf{K}(\mathbf{r})$, proportional to the Feibelman $d$ parameters, see Fig. 1(b). Together, they provide a general and first-principles approach, which transparently and accurately separates the distinct roles of shape, scale, and material down to the nanometer scale.

Several aspects remain open for exploration: for instance, the retarded generalization of this approach follows by including the same boundary terms $\pi(\mathbf{r})$ and $\mathbf{K}(\mathbf{r})$, allowing immediate incorporation, e.g., in retarded boundary element methods. Another contiguous application lies with coupled nanostructures, with implications, e.g., for plasmon rulers [69,70]. Nonclassical modifications to scattering properties [71] and their concomitant impact on classical sum rules and scattering limits [72] poses a separate open question. Moreover, beyond the perturbative

treatment emphasized here, new phenomena without a classical equivalent emerge, such as the Bennett mode [73] which corresponds to poles of $d_\perp$ [74]. Finally, the approach extends to several novel plasmonic platforms, such as highly doped semiconductors [75]—it may translate to 2D plasmonics as well, e.g., enabling analytical insight in the plasmonic properties of zigzag- vs armchair-terminated graphene nanostructures [76] through analogous nonclassical edge densities.

In conclusion, we hope these results will renew interest in the Feibelman $d$ parameters as a general tool and fundamental platform in the field of quantum nanoplasmonics.

[*] tchr@mit.edu

[†] wyanzju@gmail.com

[1] L. Genzel, T. P. Martin, and U. Kreibig, Z. Phys. B **21**, 339 (1975).

[2] F. Ouyang, P. E. Batson, and M. Isaacson, Phys. Rev. B **46**, 15421 (1992).

[3] J. Tiggesbäumker, L. Köller, K.-H. Meiwes-Broer, and A. Liebsch, Phys. Rev. A **48**, R1749 (1993).

[4] T. Reiners, C. Ellert, M. Schmidt, and H. Haberland, Phys. Rev. Lett. **74**, 1558 (1995).

[5] K.-P. Charlé, L. König, S. Nepijko, I. Rabin, and W. Schulze, Cryst. Res. Technol. **33**, 1085 (1998).

[6] J. A. Scholl, A. L. Koh, and J. A. Dionne, Nature (London) **483**, 421 (2012).

[7] K. J. Savage, M. M. Hawkeye, R. Esteban, A. G. Borisov, J. Aizpurua, and J. J. Baumberg, Nature (London) **491**, 574 (2012).

[8] S. Raza, N. Stenger, S. Kadkhodazadeh, S. V. Fischer, N. Kostesha, A.-P. Jauho, A. Burrows, M. Wubs, and N. A. Mortensen, Nanophotonics **2**, 131 (2013).

[9] S. Raza, S. Kadkhodazadeh, T. Christensen, M. Di Vece, M. Wubs, N. A. Mortensen, and N. Stenger, Nat. Commun. **6**, 8788 (2015).

[10] D. Jin, Q. Hu, D. Neuhauser, F. von Cube, Y. Yang, R. Sachan, T. S. Luk, D. C. Bell, and N. X. Fang, Phys. Rev. Lett. **115**, 193901 (2015).

[11] P. J. Feibelman, Prog. Surf. Sci. **12**, 287 (1982).

[12] W. Zhu, R. Esteban, A. G. Borisov, J. J. Baumberg, P. Nordlander, H. J. Lezec, J. Aizpurua, and K. B. Crozier, Nat. Commun. 7, 11495 (2016).

[13] S. Raza, S. I. Bozhevolnyi, M. Wubs, and N. A. Mortensen, J. Phys. Condens. Matter 27, 183204 (2015).

[14] J. B. Khurgin, Faraday Discuss. 178, 109 (2015).

[15] E. Townsend and G. W. Bryant, Nano Lett. 12, 429 (2012).

[16] E. Townsend and G. W. Bryant, J. Opt. 16, 114022 (2014).

[17] A. Varas, P. García-González, J. Feist, F. J. García-Vidal, and A. Rubio, Nanophotonics 5, 409 (2016).

[18] P. Zhang, J. Feist, A. Rubio, P. García-González, and F. J. García-Vidal, Phys. Rev. B 90, 161407(R) (2014).

[19] Time-Dependent Density Functional Theory, edited by M. A. L. Marques, C. A. Ullrich, F. Nogueira, A. Rubio, K. Burke, and E. K. U. Gross, Lecture Notes in Physics (Springer, New York, 2006).

[20] J. A. Schuller, E. S. Barnard, W. Cai, Y. C. Jun, J. S. White, and M. L. Brongersma, Nat. Mater. 9, 193 (2010).

[21] L. Novotny and N. van Hulst, Nat. Photonics 5, 83 (2011).

[22] V. Giannini, A. I. Fernández-Domínguez, S. C. Heck, and S. A. Maier, Chem. Rev. 111, 3888 (2011).

[23] W. Yan, M. Wubs, and N. Asger Mortensen, Phys. Rev. Lett. 115, 137403 (2015).

[24] C. David and F. J. García de Abajo, J. Phys. Chem. C 115, 19470 (2011).

[25] S. Raza, G. Toscano, A.-P. Jauho, M. Wubs, and N. A. Mortensen, Phys. Rev. B 84, 121412(R) (2011).

[26] C. Ciracì, R. T. Hill, J. J. Mock, Y. Urzhumov, A. I. Fernández-Domínguez, S. A. Maier, J. B. Pendry, A. Chilkoti, and D. R. Smith, Science 337, 1072 (2012).

[27] Y. Luo, A. I. Fernández-Domínguez, A. Wiener, S. A. Maier, and J. B. Pendry, Phys. Rev. Lett. 111, 093901 (2013).

[28] See Supplemental Material at http://link.aps.org/supplemental/10.1103/PhysRevLett.118.157402, for additional details, including a self-contained introduction to the $d$ parameters, full derivations of the main results, and an extended discussion of the SSA-TDDFT computation of $d$ parameters, which includes Refs. [29–43].

[29] K. Kempa and W. L. Schaich, Phys. Rev. B 34, 547 (1986).

[30] I. S. Gradshteyn and I. M. Ryzhik, Table of Integrals, Series, and Products, 7th ed. (Academic Press, New York, 2007).

[31] F. H. L. Koppens, D. E. Chang, and F. J. García de Abajo, Nano Lett. 11, 3370 (2011).

[32] J. D. Jackson, Classical Electrodynamics, 3rd ed. (John Wiley & Sons, New York, 1999).

[33] T. V. Shahbazyan, Phys. Rev. B 94, 235431 (2016).

[34] N. D. Lang and W. Kohn, Phys. Rev. B 1, 4555 (1970).

[35] A. Liebsch, Phys. Rev. B 36, 7378 (1987).

[36] E. Cottancin, G. Celep, J. Lermé, M. Pellarin, J. R. Huntzinger, J. L. Vialle, and M. Broyer, Theor. Chem. Acc. 116, 514 (2006).

[37] L. Serra and A. Rubio, Phys. Rev. Lett. 78, 1428 (1997).

[38] H.-Ch. Weissker and C. Mottet, Phys. Rev. B 84, 165443 (2011).

[39] P. J. Feibelman, Phys. Rev. Lett. 72, 788 (1994).

[40] H. Haberland, Nature (London) 494, E1 (2013).

[41] J. Yan, K. W. Jacobsen, and K. S. Thygesen, Phys. Rev. B 84, 235430 (2011).

[42] G. A. Benesh and J. E. Inglesfield, J. Phys. C 17, 1595 (1984).

[43] J. E. Inglesfield and G. A. Benesh, Phys. Rev. B 37, 6682 (1988).

[44] A. Liebsch, Electronic Excitations at Metal Surfaces, Physics of Solids and Liquids (Springer, New York, 1997).

[45] $d_\parallel$ may also be viewed as a length proportional to the integrated difference of ionic and equilibrium electron densities [46].

[46] P. Apell, Phys. Scr. 24, 795 (1981).

[47] P. Apell, R. Monreal, and F. Flores, Solid State Commun. 52, 971 (1984).

[48] A. Liebsch and W. L. Schaich, Phys. Rev. B 52, 14219 (1995).

[49] P. Apell and A. Ljungbert, Phys. Scr. 26, 113 (1982).

[50] P. Apell and A. Ljungbert, Solid State Commun. 44, 1367 (1982).

[51] The $k$ dependence of the mapping can, in principle, be retained, see Ref. [23], though at the expense of analytical accessibility.

[52] O. D. Kellogg, Foundations of Potential Theory (Springer, New York, 1967).

[53] F. Ouyang and M. Isaacson, Philos. Mag. B 60, 481 (1989).

[54] F. J. García de Abajo and J. Aizpurua, Phys. Rev. B 56, 15873 (1997).

[55] W. Yan, N. A. Mortensen, and M. Wubs, Phys. Rev. B 88, 155414 (2013).

[56] O. Schnitzer, V. Giannini, S. A. Maier, and R. V. Craster, Proc. R. Soc. A 472, 20160258 (2016).

[57] For example, for the $l$th multipole plasmon in a sphere of radius $R$, the HDM shift $\omega_{l,\mathrm{HDM}}^{(1)} = \frac{1}{2}\sqrt{l(l+1)}\beta/R$ [58] is retrieved.

[58] T. Christensen, W. Yan, S. Raza, A.-P. Jauho, N. A. Mortensen, and M. Wubs, ACS Nano 8, 1745 (2014).

[59] S. P. Apell, P. M. Echenique, and R. H. Ritchie, Ultramicroscopy 65, 53 (1996).

[60] S. Raza, T. Christensen, M. Wubs, S. I. Bozhevolnyi, and N. A. Mortensen, Phys. Rev. B 88, 115401 (2013).

[61] U. Kreibig and C. Fragstein, Z. Phys. 224, 307 (1969).

[62] U. Kreibig and L. Genzel, Surf. Sci. 156, 678 (1985).

[63] Kreibig's form is obtained by setting $d_\parallel^{(0)} = 0$ and $d_\perp^{(0)} = \sqrt{3}v_F/2\omega_p$.

[64] N. A. Mortensen, S. Raza, M. Wubs, T. Søndergaard, and S. I. Bozhevolnyi, Nat. Commun. 5, 3809 (2014).

[65] G. Weick, G.-L. Ingold, R. A. Jalabert, and D. Weinmann, Phys. Rev. B 74, 165421 (2006).

[66] O. Gunnarsson and B. I. Lundqvist, Phys. Rev. B 13, 4274 (1976).

[67] A. Liebsch, Phys. Rev. B 48, 11317 (1993).

[68] P. B. Johnson and R. W. Christy, Phys. Rev. B 6, 4370 (1972).

[69] T. V. Teperik, P. Nordlander, J. Aizpurua, and A. G. Borisov, Phys. Rev. Lett. 110, 263901 (2013).

[70] T. V. Teperik, P. Nordlander, J. Aizpurua, and A. G. Borisov, Opt. Express 21, 27306 (2013).

[71] To leading order, the dipole polarizability $\alpha$ generalizes to

$$\alpha = 2\sum_n \frac{\alpha_n^{(0)} + d_\alpha \alpha_{\alpha,n}^{(1)}}{\Lambda_n^{(0)} + d_\alpha \Lambda_{\alpha,n}^{(1)} - \Lambda} + \mathcal{O}(d_\alpha^2),$$

with oscillator strengths (induced along $\hat{\mathbf{i}}$, perturbed along $\hat{\mathbf{j}}$)

$$\alpha_n^{(0)} \equiv \frac{\langle \phi_n^{(0)} | \hat{\mathbf{n}} \cdot \hat{\mathbf{j}} \rangle \langle \mathbf{r} \cdot \hat{\mathbf{i}} | \sigma_n^{(0)} \rangle}{\langle \phi_n^{(0)} | \sigma_n^{(0)} \rangle},$$

$$\alpha_{\alpha,n}^{(1)} \equiv \frac{\langle \phi_n^{(0)} | \mathsf{V}_\alpha \mathsf{P}_n | \hat{\mathbf{n}} \cdot \hat{\mathbf{j}} \rangle \langle \mathbf{r} \cdot \hat{\mathbf{i}} | \sigma_n^{(0)} \rangle}{\langle \phi_n^{(0)} | \sigma_n^{(0)} \rangle},$$

and weighted projection operator $\mathsf{P}_n \equiv \sum_{n' \neq n} \frac{1}{\Lambda_{n'}^{(0)} - \Lambda} \frac{|\sigma_{n'}^{(0)}\rangle\langle\phi_{n'}^{(0)}|}{\langle\phi_{n'}^{(0)}|\sigma_{n'}^{(0)}\rangle}$.

[72] O. D. Miller, C. W. Hsu, M. T. H. Reid, W. Qiu, B. G. DeLacy, J. D. Joannopoulos, M. Soljačić, and S. G. Johnson, Phys. Rev. Lett. **112**, 123903 (2014).

[73] A. J. Bennett, Phys. Rev. B **1**, 203 (1970).

[74] K.-D. Tsuei, E. W. Plummer, A. Liebsch, E. Pehlke, K. Kempa, and P. Bakshi, Surf. Sci. **247**, 302 (1991).

[75] A. M. Schimpf, N. Thakkar, C. E. Gunthardt, D. J. Masiello, and D. R. Gamelin, ACS Nano **8**, 1065 (2014).

[76] T. Christensen, W. Wang, A.-P. Jauho, M. Wubs, and N. A. Mortensen, Phys. Rev. B **90**, 241414(R) (2014).